

# Shear flow in compound channels

**J. N. V. Goulart**

PROMEC – Universidade Federal do Rio Grande do Sul  
[jhongoulart@yahoo.com.br](mailto:jhongoulart@yahoo.com.br)

**S. V. Möller**

PROMEC – Universidade Federal do Rio Grande do Sul  
[svmoller@ufrgs.br](mailto:svmoller@ufrgs.br)

Rua Sarmento Leite, 425 – Porto Alegre – Rio Grande do Sul – Brasil  
Porto Alegre – Rio Grande do Sul, Brasil  
cep: 90050 – 170

***Abstract:** The purpose of this paper is the experimental investigation of large scale structures in the shear flow in compound channels. Compound channels are found in the nuclear and process industry, in channels like rod bundles, heat exchangers and coolers of modern electronic devices. The geometrical characteristics of the channels generate velocity profiles with very high vorticity values, which give origin to large scale structures, responsible for convective heat transfer enhancement, mixing and to the possibility of inducing vibration of the structures. By means of hot wire anemometry the flow in a test section is investigated. This consisting of two parallel plates placed on a wall of a wind channel, forming a slot with width “d” and depth “p”. The working fluid is air. Ten different p/d configurations were studied. Results allow the determination of the flow characteristics of the shear layer formed in the interior of the slot as well as most representative scales for the definition of the Strouhal number.*

*Keywords:* compound channels, coherent structures, hot wires

## 1 Introduction

Compound channels are characterized by the presence of a narrow region connecting two main channels, like in rod bundles of nuclear reactors, where two adjacent subchannels are connected by the narrow gap between the rods, Möller, 1991. The flow in the gap region has pulsating characteristics responsible for mass and momentum exchange between the subchannels, due to the presence of large-scale structures, which are transported by the main flow. These structures are responsible for increasing the Reynolds stresses in the boundary region between the gap (or slot) and the main channel. The work of Meyer and Rehme, 1995, and the work of Soldini et al., 2004, show that this kind of phenomenon of flow pulsations appears not only in rod bundles of nuclear reactors, but also in heat exchangers (tube banks), coolers of electronic devices and irrigation channels.

Flow pulsations in rod bundles were first reported by Rowe et al., 1974 where the axial component of the velocity fluctuation presented periodical characteristics. The frequency associated to this phenomenon increased when the distance between the rods was reduced. In the work of Möller, 1991, hot wire anemometry was employed to determine the origin and characteristics of this phenomenon. The results demonstrated that the flow pulsations were associated to the strong vorticity field near the gaps and that the dimensionless frequency in form of a Strouhal number was a function of the geometry of the channel. The Strouhal number was defined with the rod diameter and the friction velocity in the narrow gap between the rods.

Although a significant number of experimental works about the flow in rod bundles have been published since then, the conclusions about the definition of a Strouhal number and correlations able to describe precisely the frequency of the pulsation are not unanimous, these being based on geometrical and flow parameters. Wu and Trupp, 1994, performed hot wire measurements in a trapezoidal channel containing a single tube. The results showed pronounced peaks in spectra, confirming the strong dependence of the frequency on geometrical parameters and the flow velocity, but the values of the Strouhal number obtained did not agree with the correlations proposed by Möller, 1991, leading the Authors to suggest a new correlation for the determination of the Strouhal number.

Meyer and Rehme, 1995, using hot wire anemometry studied the flow characteristics in a channel with two or several parallel plates attached to a wall in geometry similar to an internally finned channel, so that one or more narrow channels were connected to a wider one, and in a test section formed by two rectangular channels connected by a slot. The parallel plates geometry had values of the geometrical parameter  $d/g=1.66$  to  $d/g=10.0$ , being  $d$  the depth of the slot formed by the plates and  $g$  the distance between two plates. Authors observed the presence of large scale structures producing flow pulsations for  $d/g \geq 2$  confirmed by flow visualizations experiments for Reynolds numbers as low as  $Re=150$ . A correlation for the Strouhal number is proposed based on the velocity measured in the edge of the plates, and the square root of the product of “d” and “g”, but the results showed errors for  $d/g$  values greater than 7.

Guellouz and Tavoularis, 2000, used hot wires and flow visualizations to investigate flow pulsations in a rectangular channel containing a single tube. The results showed the predominance of these structures in the region near the gap between tube and channel wall even for relatively large values of the gap spacing, confirming results by Meyer and Rehme, 1995, who showed that the transport velocity of the vortices and the spacing between them is a function of the gap size.

The purpose of this work is, therefore, to investigate the presence of flow pulsations in compound channels formed by two parallel plates attached to a wall in a fin-like geometry and their formation conditions, as well as to obtain velocity and length scales for the definition of a Strouhal number.

## 2 Test Section and Experimental Technique

The test section consists on a 3320 mm long channel and 146 mm height and a variable width,  $w$ . Three different values were adopted, namely 60, 120 and 150 mm. Working fluid was air at room temperature, driven by a centrifugal blower controlled by a frequency inverter, reaching the test section after passing through a diffuser and a set of honeycombs and screens with about 1% turbulence intensity. After the screens a Pitot tube placed on a fixed position was used to measure the reference velocity  $U_{ref}$  of the experiments, which had a constant value of  $U_{ref}=13.50$  m/s ( $\pm 0.1$  m/s) for all experiments.

Inside the channel two metal plates with thickness  $e = 1.2$  mm and length “L” were mounted onto a side wall to form a canyon like slot with depth “p” and width “d”. Table 1 shows the dimensions of the test sections and the Reynolds numbers of each test section. Reynolds numbers were defined with the reference velocity,  $U_{ref}$ , and the hydraulic diameter channels,  $D_h$ .

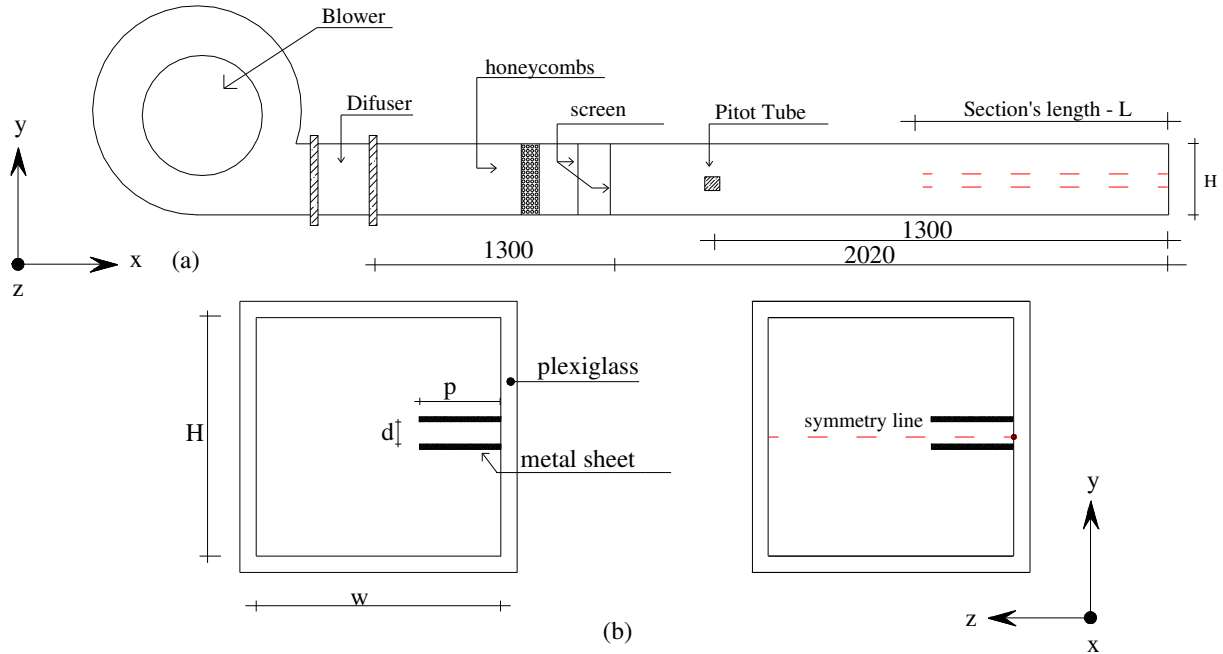


Figure 1 – Schematic view of the test section (a) and cross sectional (b) view with plates and geometrical parameters.

Table 1 – Test section configurations and Reynolds number – (Dimensions in mm).

Test section #	w	p	d	L	p/d	w/p	$Re = \frac{U_{ref} \times D_h}{\nu}$
01	150	50	10	1250	5	3	$14.90 \times 10^3$
02	120	40	8	1000	5	3	$11.01 \times 10^3$
03	60	20	4	500	5	3	$7.40 \times 10^3$
04	150	50	10	500	5	3	$13.01 \times 10^3$
05	120	40	8	500	5	3	$13.51 \times 10^3$
06	60	20	4	250	5	3	$7.30 \times 10^3$
07	150	50	4	1250	12.5	3	$16.50 \times 10^3$
08	120	40	4	1000	10	3	$13.60 \times 10^3$
09	150	50	4	500	12.5	3	$13.00 \times 10^3$
10	120	40	4	500	10	3	$12.60 \times 10^3$

Measurements of velocity and velocity fluctuations were performed by a hot wire DANTEC *StreamLine* system using a double wire probe with a slant wire ( $45^\circ$ ) and a wire perpendicular to the main flow to perform simultaneous measurements of the transversal ( $w$  – parallel to the symmetry line, Fig. 1-b) and axial components ( $u$ ) of the velocity vector. Collis and Williams, 1959, method with modifications by Olinto and Möller, 2004 was applied for the evaluation of the anemometer signals. Velocity field was previously measured by a Pitot tube. Measurements were performed 20 mm before channel outlet.

Data acquisition was performed by means of a 12 bit Keithley DAS58 A/D converter board, with a sampling frequency of 3 KHz and a low pass filter set at 1 KHz. Length of time series was 43.69 s.

### 3 Results and discussion

#### 3.1 Velocity profile

Figure 2 presents the velocity distribution along the symmetry line of test section #. 2 (Table 1). There, the width of the parallel plates, or depth of the slot, is indicated by the value of  $p$ . The velocity profile can be divided in three different zones: while in zones 1 and 3 velocity distribution is strongly influenced by the walls on the extremities of symmetry line, zone 2 has the characteristics of a mixing layer beginning in the region between the plates and extending towards the main flow. The mixing layer formation in compound channels was related by Shiono and Knight, 1991, when the authors performed measurements in an open channel with flooding plains.

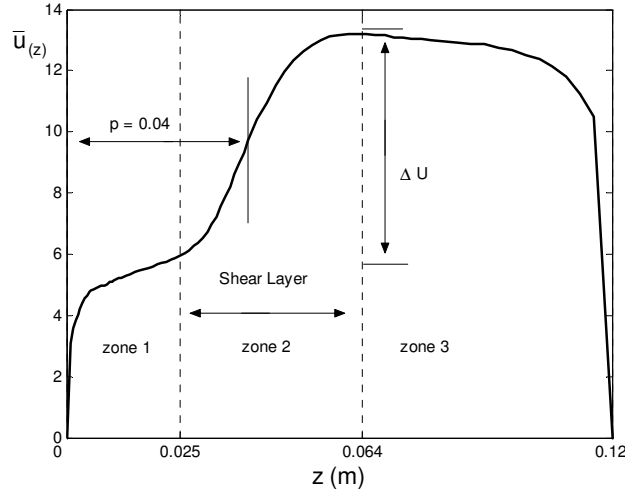


Figure 2 – Axial velocity profile on the symmetry line, section # 2.

Figure 3 presents the mean axial velocity distribution along the symmetry line for test sections # 01 to 06 (Table 1). In general the same features of Fig. 2 can be observed for all cases studied. Can be observed, through the velocity profiles, a mixing layer formation that are clearly defined, mainly for test section from 01 to 03, where there are two different velocity layers, with a maximum velocity  $U_2$  and minimum velocity  $U_1$ . Nevertheless, in Figure 3 (b) the mixing layer features are not so clear, and the velocity profiles show a still developing flow.

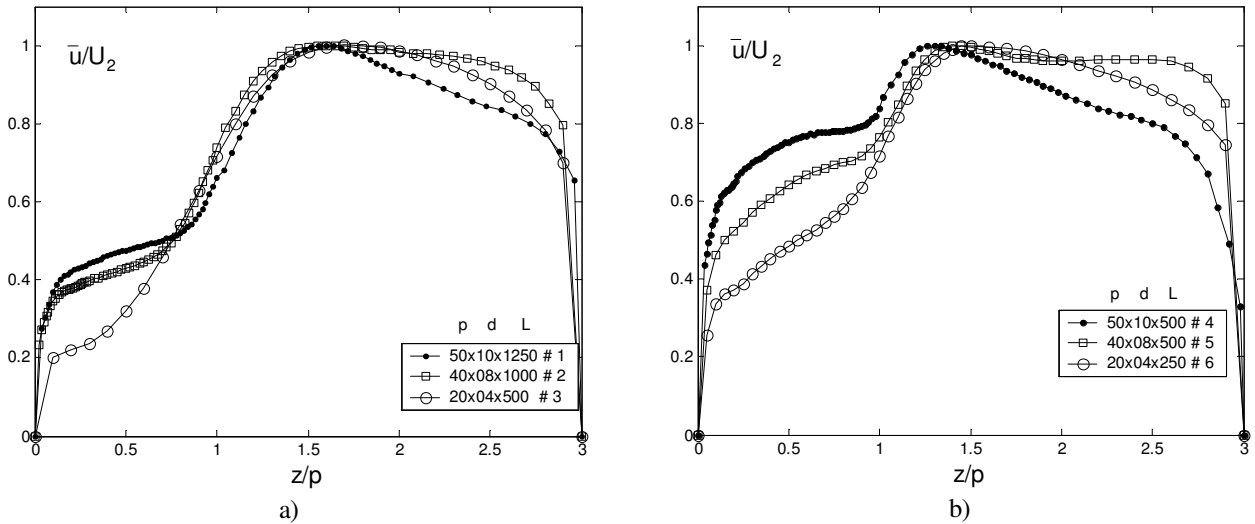


Figure 3 – Axial velocity distribution along the symmetry line: a) test sections 1, 2 and 3; b) test sections 04, 05 and 06.

For better comprehension of the phenomenon, velocity values were normalized by the maximal velocity in the shear layer, while the  $z$ -coordinate was normalized by the depth of the narrow part of the channel,  $p$ .

How all the velocity profiles show only one maximum velocity point, it is easy to determine the maximum mixing layer velocity,  $U_2$ , in spite of this fact, only by observing Fig. 3, the value of the minimum velocity,  $U_1$ , cannot be inferred. Therefore, the velocity gradient will be used to determine the position of the end wall influence and the beginning of the shear layer. The minimum velocity,  $U_1$ , is defined as the velocity value where the velocity gradient changes its concavity, so at this position,

$$\left. \frac{\partial^2 \bar{u}}{\partial z^2} \right|_{U_1} = 0 \quad (1)$$

where the first derivative, is calculated by forward differences.

In Fig. 4, dimensionless velocity and velocity gradients are plotted as a function of the dimensionless coordinate  $z/p$ . In all test sections investigated, an inflexion point near the edge of the narrow part of the channel is found the vertical lines show the upper and lower velocities location,  $U_2$  and  $U_1$ , in the mixing layer.

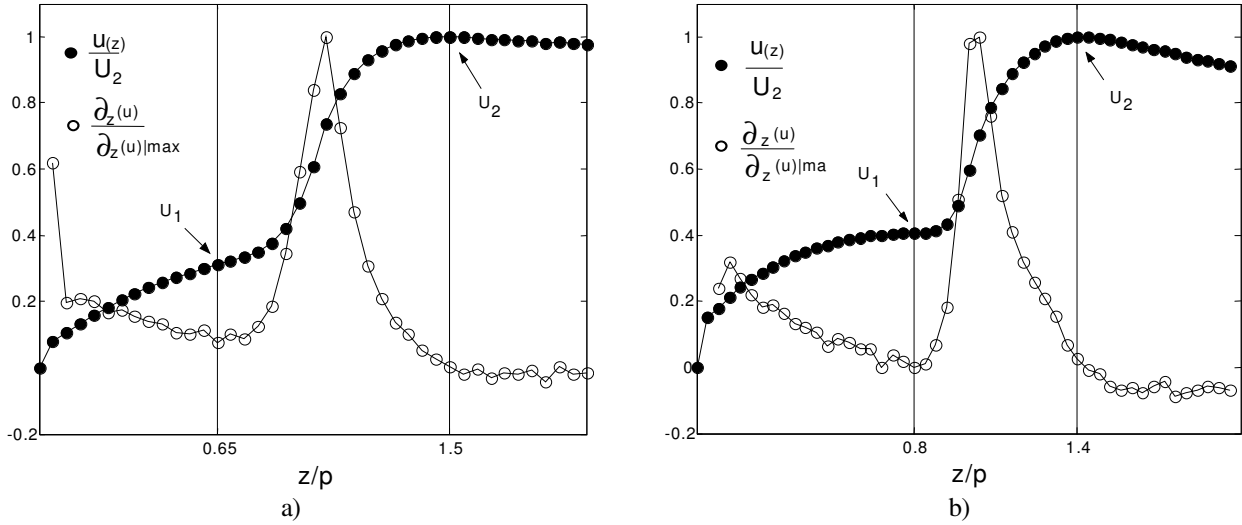


Figure 4 – Gradients and velocity profiles: a) test section #10. b) test section #9.

### 3.2 Velocity distribution in shear layers

Since, there is a mixing layer and this one extends from somewhere between the plates to a certain position into main channel, it is possible to figure out this problem as a steady state planar turbulent mixing layer in spatial development, where the momentum equation is written as

$$u \frac{\partial u}{\partial x} + w \frac{\partial u}{\partial x} = \nu_t \frac{\partial^2 u}{\partial z^2} \quad (2)$$

where  $u$ ,  $w$ , are axial and transversal velocity components respectively and  $\nu_t$  is an eddy-viscosity.

So, the self-similar solutions can be found as

$$\bar{u}_{(z)} = U_c + \Delta U f(\eta) \quad (3)$$

where:

$\Delta U$  = difference between the lower and the upper velocities in the mixing layer,  $U_1$  and  $U_2$ , respectively;  
 $U_c$  = convection velocity, defined by

$$U_c = \frac{U_2 + U_1}{2} \quad (4)$$

$\eta$  = similarity parameter, defined according to Prooijen and Uijttewaal, 2002, by

$$\eta = 2 \times \frac{z - z_c}{\delta_{(x)}} \quad (5)$$

where

$z_c$  = coordinate of the center of the mixing layer;

$\delta_{(x)}$  = thickness of the mixing layer, defined as

$$\delta_{(x)} = \frac{U_2 - U_1}{(\partial u / \partial z)_{\max.}} \quad (6)$$

According to Lesieur, 1997, the self-similar solution for the eq. (3), leads to an error function for the mixing layer velocity profile, however, a hyperbolic tangent function ( $\tanh$ ) is widely used, thus

$$\bar{u}(\eta) = \frac{\Delta U}{2} \left( \frac{2}{\lambda} + \tanh(\eta) \right) \quad (7)$$

The velocity ratio,  $\lambda$ , is defined as a difference velocity,  $\Delta U$  and convection velocity  $U_c$ , ratio, given by

$$\lambda = \frac{2\Delta U}{U_2 + U_1} \quad (8)$$

The velocity ratio,  $\lambda$ , is also called as rate of shear as showed by Yang et al., 2004, and depicts the relationship between the main characteristic of a mixing layer, its velocity difference, and the velocity of the center mixing layer. It can imagine, at the beginning, before reaching test sections, the velocity profile is fitted as logarithmic function, then when the flow enter into the test section the velocity profile changes and the velocity difference start being established increasing along streamwise. Therefore, only by using the velocity difference is not possible to realize the influence of this feature in the velocity profile being required another velocity scale in order to make a dimensionless number in form of velocity ratio,  $\lambda$ .

Figure 5 shows the velocity profiles of test sections #3 and #7. Experimental data were plotted as a function of the similarity parameter  $\eta$ , Eq. (5). The use Eq. (7) with the hyperbolic tangent function for the velocity profile (Lesieur, 1997) presents a good agreement with the experimental data in all test sections investigated. However, for the test sections where the velocity difference inside the shear layer is small, there are very few experimental data points of the velocity profiles, as, for example, test section #6, where the determination of the lower velocity  $U_1$  was very difficult.

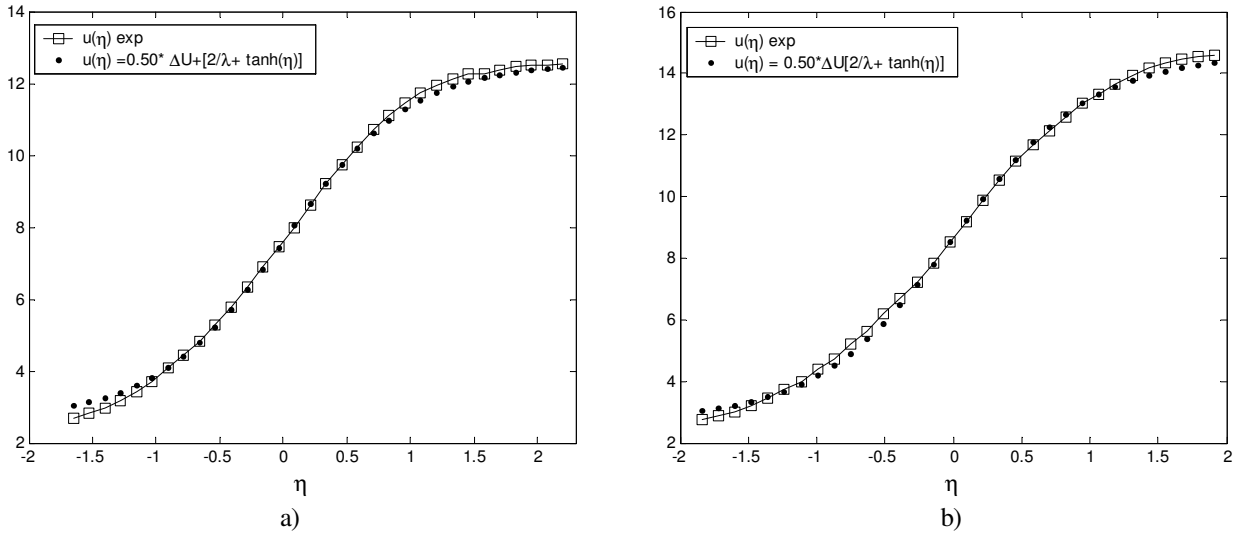


Figure 5 – Mean axial velocity distribution in to the mixing layer and its approximation by hyperbolic tangent function. a) section #3. b) section #7.

### 3.3 The shear layer thickness

Self-similarity is a state of local equilibrium where the flow quantities are only dependent upon local variables, including mean velocities and its fluctuations, as well as local length scales, such as width shear layer,  $\delta$ , and momentum thickness,  $\theta$ . Once self-similarity was achieved these local lengths depend on streamwise position, which were obtained. In theory is expected a linear mixing layer growing with the streamwise coordinate in the self-similar state. Indeed, Figure 6, shows the relationship between mixing layer thickness,  $\delta$ , and the section test length, as observed, through the curves, A and B, mixing layer width increases as a linear function of the test sections length, implying the self-similar state has been accomplished. However, must be observed important differences about the growing mixing layer rates.

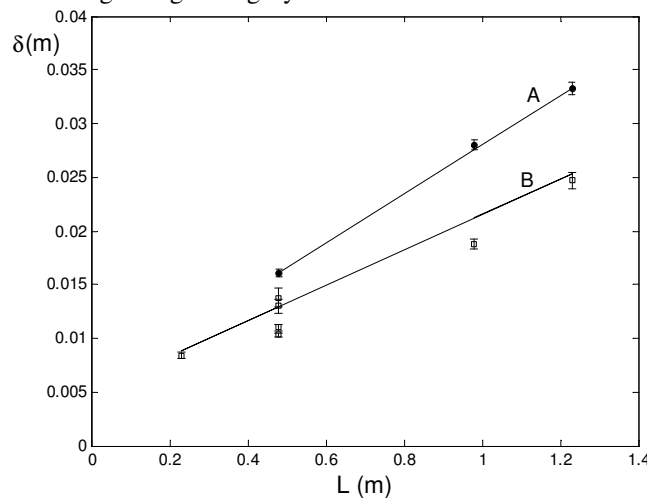


Figure 6 – Growth of mixing layer with the increasing section test length.

The upper curve, A, shows a bigger growth rate than curve B,  $d\delta/dL = 0.023$  and  $0.0165$ , respectively. In this case, the difference between the two growth rates is about 40%. This fact was reported on Bell and Mehta, 1990, and Yang et al., 2004. According to authors the faster mixing layer width increase, can be explained by the streamwise vortex development. In fact, the points on curve (A), which represent test sections (Table 1), showed periodical velocity fluctuation patterns, suggesting the coherent structures presence. Therefore, the presence of coherent structures in the flow will be discussed later.

### 3.4 Reynolds stresses distribution

The profiles for the Reynolds normal stresses ( $\overline{u'^2}$ ,  $\overline{w'^2}$ ) and the shear stress,  $\overline{u'w'}$ , are presented in Figs. 6-9. The values are made dimensionless by the velocity difference ( $U_2 - U_1$ ), and plotted in similarity coordinates. The results showed here, are rather similar which ones stressed on Townsend, 1976, in classical mixing layer problems.

The Reynolds normal stresses and the shear stress distributions showed the same behavior for all cases, reaching the maximum value at the center of mixing layer,  $\eta = 0$ , and after a quick decrease towards the main channel. These features agree with the results obtained by Aubrum et al., 2002 and Yang, et al., 2004.

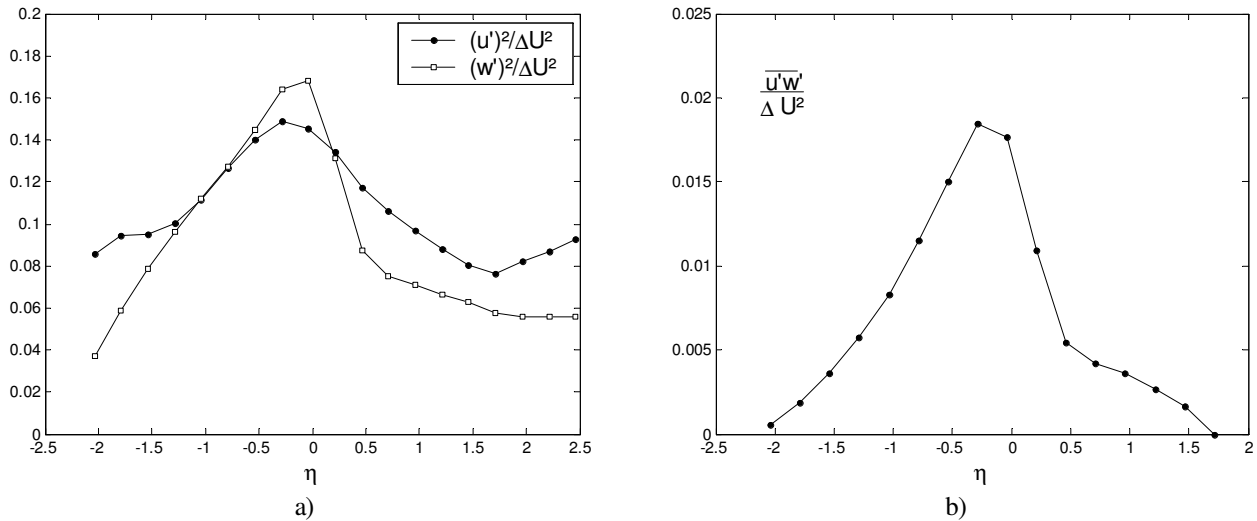


Figure 6 – Profiles of Reynolds normal stresses and shear stress, section test # 3.

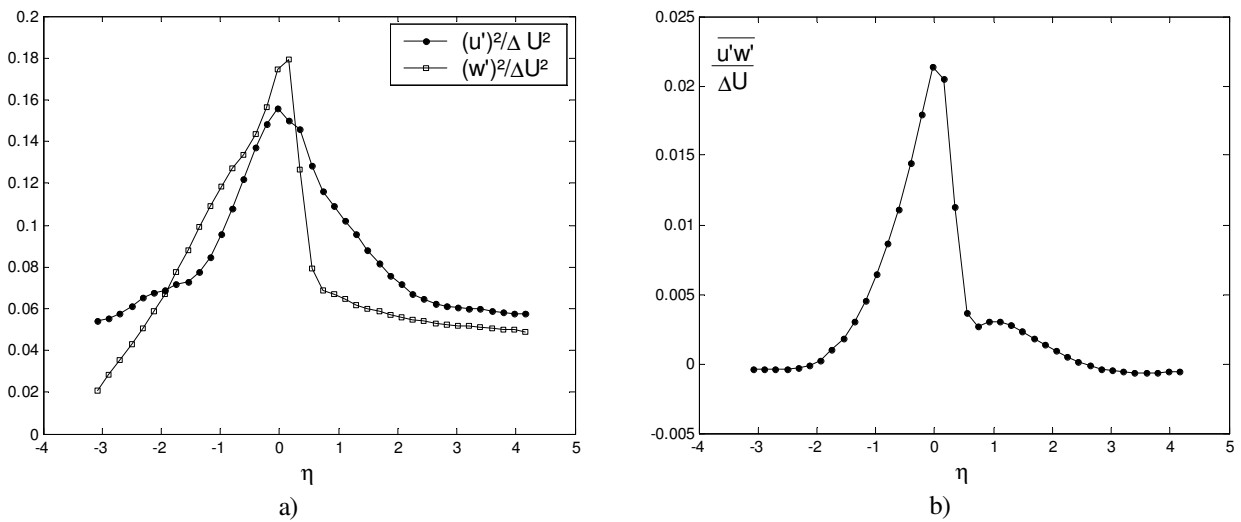


Figure 7 - Profiles of Reynolds normal stresses and shear stress, section 40x4x1000.

As regards to the peak Reynolds stresses and shear stress, they agree with the data obtained by Yang et al., 2004, in spite of present difference for the test sections # 04, 05 and 06, Figs. 8 -9. In these sections, the maximum shear stress, are higher than for others test sections.

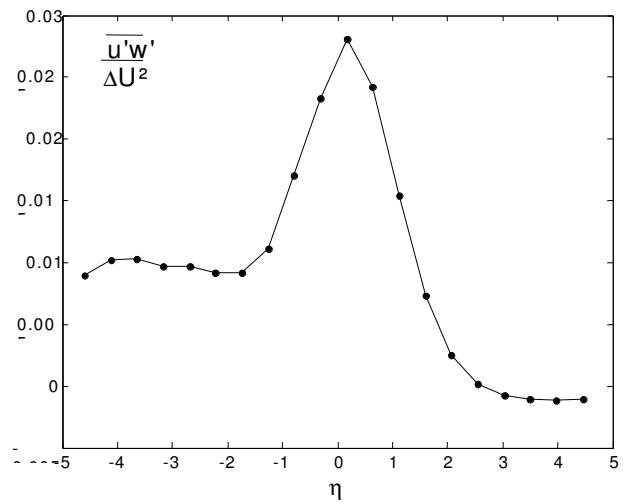
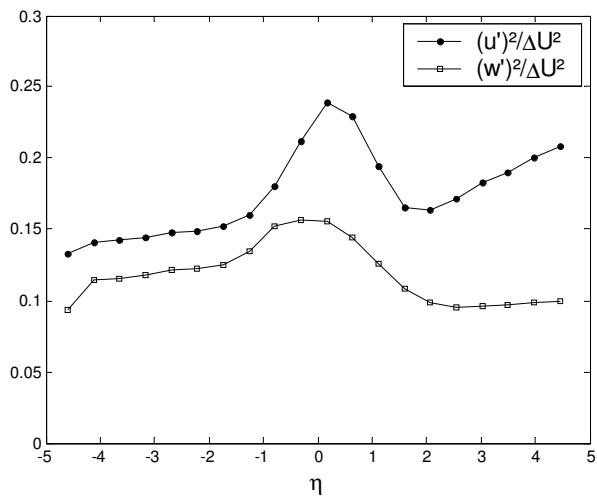


Figure 8 - Profiles of Reynolds normal stresses and shear stress, section 20x4x250.

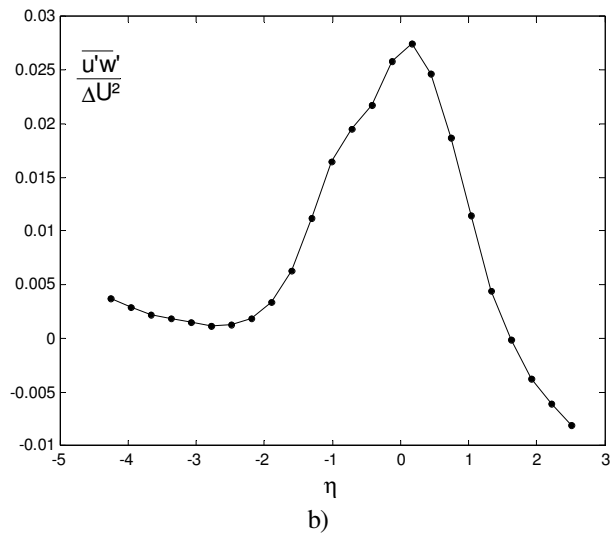
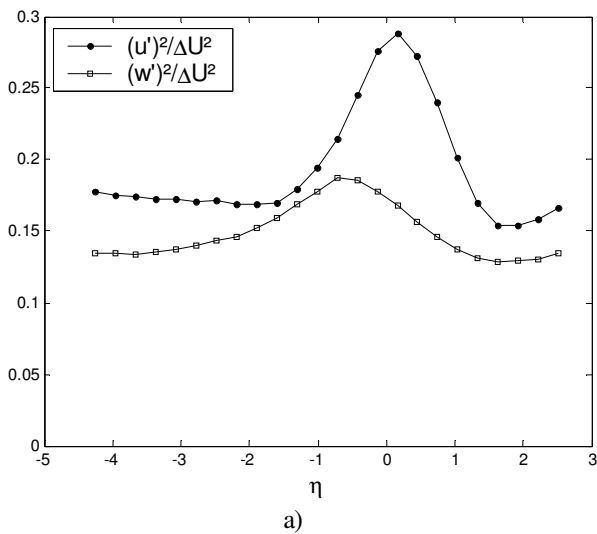


Figure 9 - Profiles of Reynolds normal stresses and shear stress, section 50x10x500.

### 3.5 The coherent structures in the flow

Another noteworthy feature in developing mixing layers concerns the streamwise vortex formation, according Bonnet and Delville, 2001, the coherent structures, in these kind of the flows, has been well known for at least the last two decades. The identification and their characterization have been done for several purposes. First, from the energetic view point. Secondly, because the dynamical properties, coherent structures play an essential role in mixing processes, drag, noise emission, heat transfer, and others diffuses process.

Figures 9 to 10 show the autospectral densities function for the both velocity components. The position, where the series were carry out, and the frequencies are done dimensionless by means similarity coordinate “ $\eta$ ” and the Strouhal number, respectively.

The Strouhal number is defined by eq. (9), such as showed by Bonnet et al., 1998, the axial and transversal velocity components were noticeable are by  $\phi_u$  and  $\phi_w$ , respectively, tha do not make dimensionless.

$$\text{Str} = \frac{f \times \delta_{(x)}}{U_c} \quad (9)$$

Where “ $f$ ” is the fundamental frequency in the autospectral density function.

For all autospectral densities function, the bandwidth is the same,  $Be = 2.92$  Hz, and the error in the Strouhal number is from 3 to 7%.

Figure 9 (a), (b) e (c), shows the autospectral densities functions for both velocity fluctuation components carried out at the mixing layer center, for the test sections # 03, 07 and 08. These test sections presents the highest velocity ratio, for their cases,  $\lambda = 1.29$ ,  $\lambda = 1.36$  and  $\lambda = 1.26$ , respectively. The autospectral densities show only one important peak and placed in the same Strouhal number, 0.17 along the symmetry line in the mixing layer. However, as such observed by Meyer and Rehme, 1994 and

Meyer e Rehme, 1995, the periodic characteristics of the velocities series, seems vanish, for the measurements carry out further edge plates.

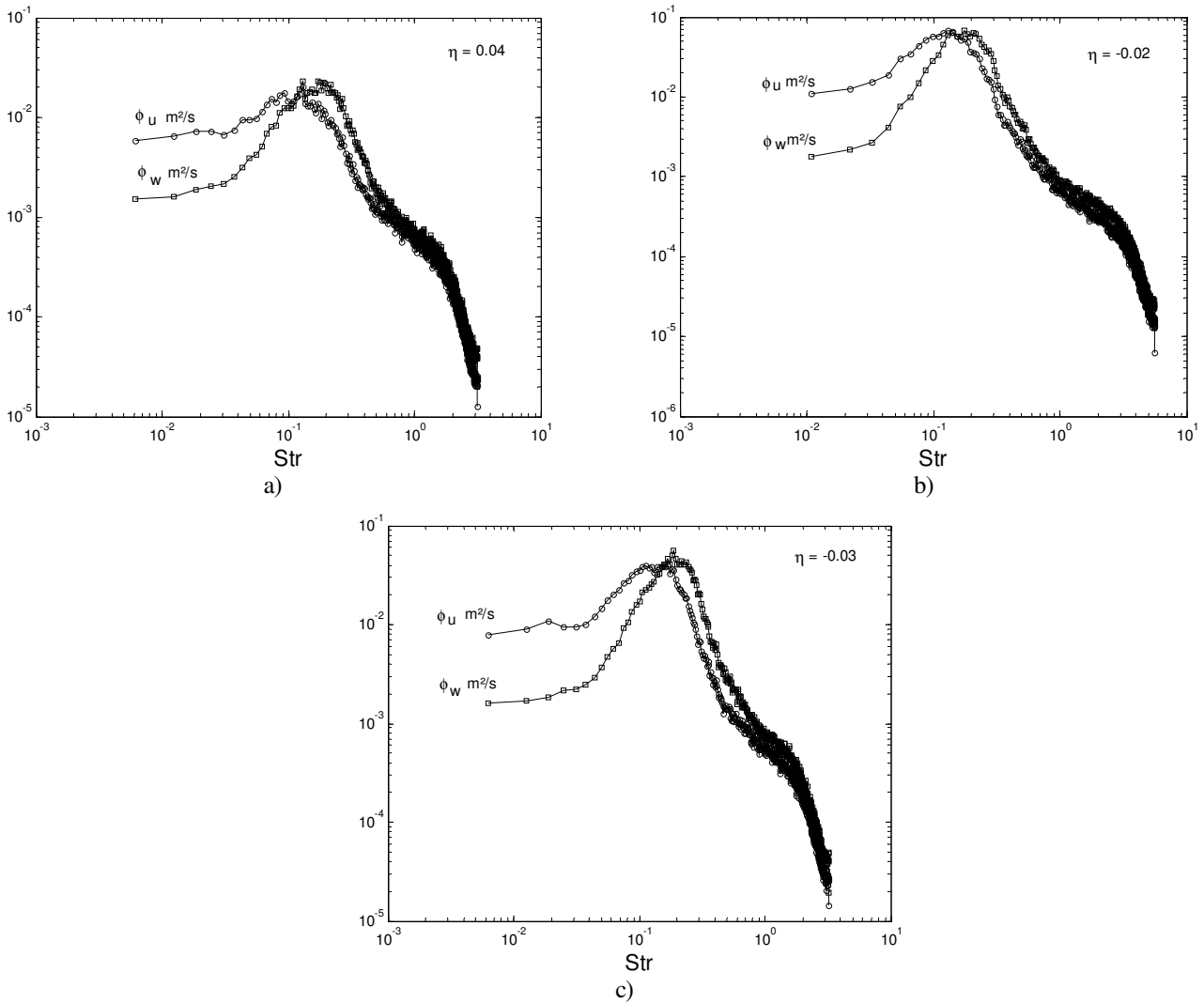
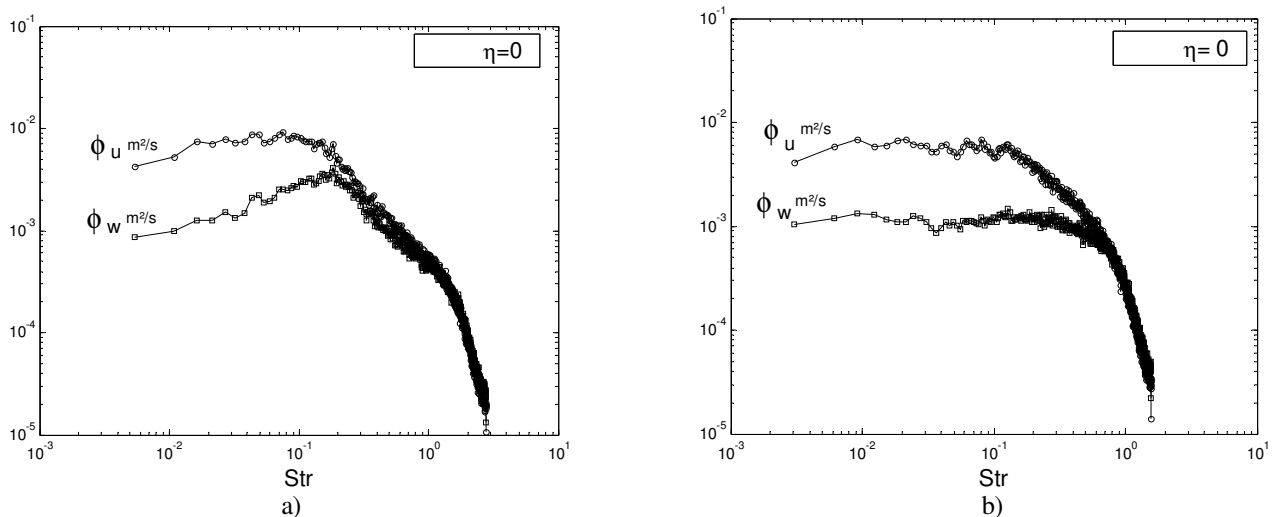


Figure 9 – Autospectral densities function for the both velocity components. a) test section # 03. b) test section # 07. c) test section # 08

On the other hand, the test sections that present a velocity ratio lower than one,  $\lambda < 1$ , the velocity fluctuations series showed no periodic behavior. In some test sections, there are small peak, fig. 11(a), which appear only the transversal velocity component and are much lower than those measured in the test sections # 03, 07 and 08. These results lead to the conclusion that the peaks in spectra, that represent streamwise vortex, are produced by the fluid flow development, it means, might exist an especial relationship between the geometrical parameters,  $p$ ,  $d$  and  $L$ , that can enable a faster development flow in test section, and thus, the large scale structures formation.





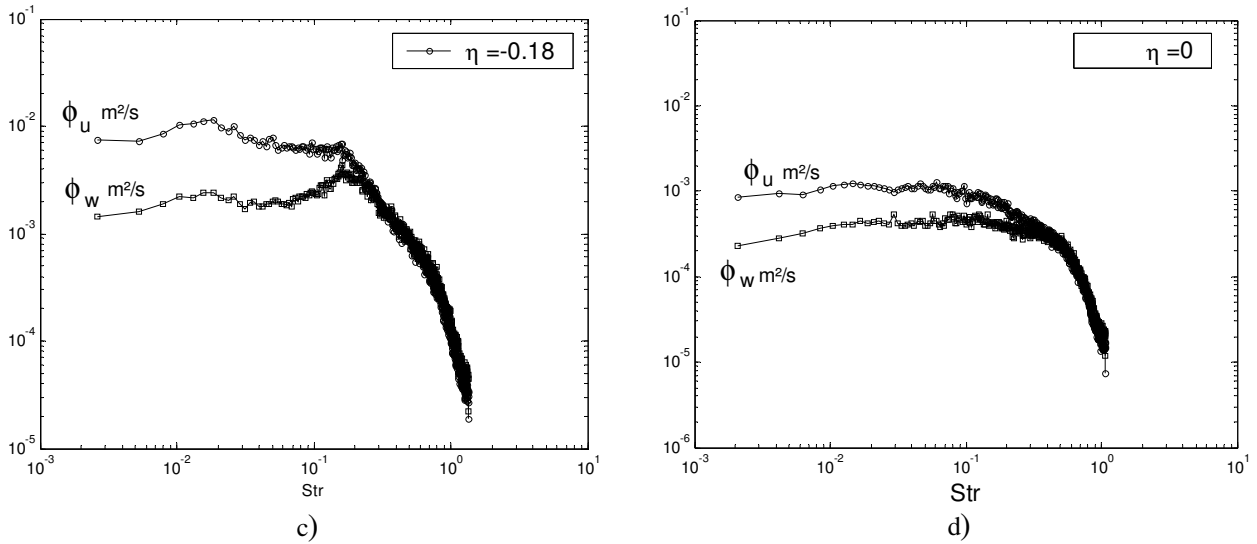


Figure 10 - Autospectral densities function for the both velocity components. a) test section

Figure 11(a), shows the behavior of Strouhal number in both velocity components, and its relationship between non-dimensional parameter  $\delta_{(x)}/d$ . The transversal Strouhal numbers distribution showed a constant behavior and well defined in  $Str_w = 0.17$ , despite axial component,  $Str_u$ , which seem to grow with the  $\delta_{(x)}/d$  ratio. Nevertheless, due the few results, about axial Strouhal number growing, a generic conclusion can not be formalized.

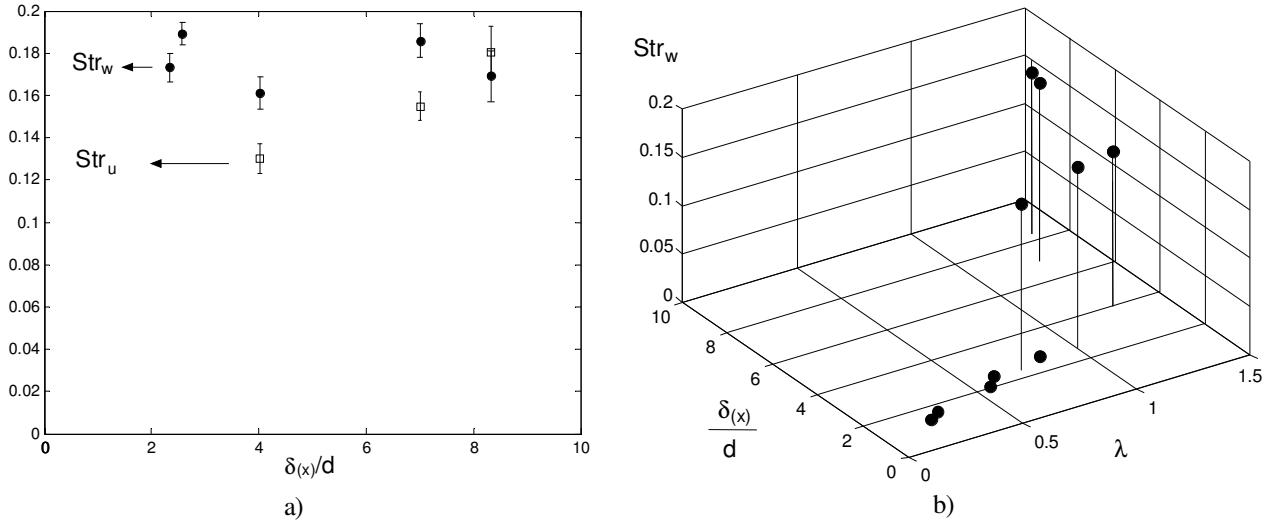


Figure 11 – Relationship between the Strouhal numbers and flow developing parameters.

As regards to Figure 11 (a), it suggests that the presence of large scale structures in the flow no longer depend of the  $p/d$  ratio, such as showed by Meyer and Rehme, 1994, but a new dimensionless parameter,  $\delta_{(x)}/d$ . Since the presence of peaks in spectra were observed in the test sections n # 02 and 03 despite test sections from n # 01 to 06 have the same  $p/d$  ratio.

The relationship between the velocity ratio,  $\lambda$ ,  $\delta_{(x)}/d$  ratio and the coherent structures observation in the flow, are showed in the Figure 11 (b). It can be observed that were not found important peaks for  $\delta_{(x)}/d$  ratio below two, and a low  $\delta_{(x)}/d$  ratio, leads a low velocity ratio.

#### 4 Concluding remarks

In this paper, an experimental study of mean and fluctuating velocities of the turbulent flow in compound channels formed by a narrow channel connected to a wider one is presented. The purpose was the investigation of flow the characteristics with a view of the presence of coherent structures with give rise to a phenomenon of quasi-periodic flow pulsations and the determination of the scales for the definition of the Strouhal number to describe the main frequency of this phenomenon.

The results of the velocity measurements showed the presence of a shear layer where the distribution of mean and fluctuating quantities showed to be functions of the measurement position only, evidencing the self preserving characteristics of the flow.

It was observed that the velocity ratio  $\lambda$  plays an important role in the dynamics of the flow, so that strong periodic characteristics, evidenced by peaks in frequency spectra, were present when the value of  $\lambda$  was greater than 1. This did not happen for values lower than one. No peaks were also observed in the regions outside the shear layer. Experimental results evidenced that the raise in the velocity ratio of the main flow is a consequence of increasing the value of the relation between the shear layer thickness,  $\delta_{(x)}$ , and the distance between the plates,  $d$ .

A Strouhal number, defined with the frequency of the transverse component of the velocity fluctuation, the convection velocity and the shear layer thickness, lead to satisfactory results, showing that these scales are representative of the flow characteristics. This Strouhal number, from all the spectra where peaks were present, had values about  $Str=0.17$ , lower than the value of 0.2 found by Bonnet et al., 1998, in their study of free shear layers. This definition for the Strouhal number appears to be very consistent and the value of  $Str = 0.17$  appears even in deep test section configurations as n #. 09 and 10, where p/d-values were 10 and 12.5, respectively.

As regards a possible growth of the Strouhal number values, inferred by the frequency peak in the axial component, the small number of experimental data does not allow any conclusion, being, therefore, necessary new experiments to describe its behavior.

## 5 Acknowledgements

The support by the CNPq – Brazilian Scientific and Technological Council is grateful acknowledged. Jhon N. V. Goulart thanks also the CNPq for granting him a fellowship.

## 6 References

- Aubrun, S., Boisson, H. C. and Bonnet, J. P., Further characterization of large-scale coherent structure signatures in a turbulent-plane mixing layer, *Experiments in Fluids*, 32, 136-142, 2002.
- Bell, J.H., Mehta, R. D., Developed of two\_stream mixing Layer from tripped and untripped boundary layers, *AIAA Journal*, v. 28, pp: 2034-2042,1990.
- Bonnet, J. P., Delville, J., Glauser, M. N., Antonia, R. A., Bisset, D. K., Cole, D. R., Fiedler, H. E., Garem J. H., Hilberg, H., Jeong, J., Kevlahan, N. K. R., Ukeiley, L. S., Vincendeau, E., Collaborative testing of eddy structure identification methods in free turbulent shear flows, *Exp Fluids* 25: 197-225, (1998).
- Bonnet, J. P., Delville, J., Review of coherent structures in turbulent free shear flows and their possible influence on computational methods, *Flow, Turbulence and Combustion*, 66, 333-353, 2001.
- Prooijen, B. C. van and Uijtewaal, W. S. J., A linear approach for the evolution of coherent structures in shallow mixing layers, *Physics of Fluids*, v. 14, pp. 4105-4114, 2002.
- Collin, D. C. and Willans, M. J., Two-dimensional convection from heated wires at low Reynolds numbers, *J. Fluid Mech.* 6 (1959) p. 357.
- Guellouz, M.S. and Tavoularis, S., The structure of the turbulent flow in a rectangular channel containing a single rod – Part 1: Reynolds-Average measurements, *Exp. Thermal and Fluid Sci.*, 23, 59-73, 2000.
- Lesieur, M., *Turbulence in Fluids*. Third Edition, Kluwer Academic Publishers, Dordrecht, The Netherlands, 1997.
- Meyer, L. and Rehme, K., Large-scale turbulence phenomena in compound rectangular channels, *Exp. Thermal Fluid Sci.*, 8, 286-304, 1994.
- Meyer, L. and Rehme, K., Periodic vortices in flow through channels with longitudinal slots or fins, 10<sup>th</sup> Symposium on turbulent shear flows, The Pennsylvania State University, University Park, August 14-16, 1995.
- Möller, S. V., On Phenomena of Turbulent Flow Through Rod Bundles. *Experimental Thermal and Fluid Science*, v. 4, n.1, pp. 25-35, 1991.
- Olinto, C. R. and Möller, S. X-probe calibration using Collis and William's equation. In: 10<sup>o</sup> Congresso Brasileiro de Engenharia e Ciências Térmicas - ENCIT, 2004, Rio de Janeiro, 2004.
- Rowe, D.S., Johnson, B.M. and Knudsen, J. G., Implications concerning rod bundle crossflow mixing based on measurements of turbulent flow structure, *Int. J. Heat Mass Transfer*, 17, 407-419, 1974.
- Shiono, B., K. and Knight, D., W. Turbulent open-channel flows with variable depth across the channel, *J. Fluid Mech.* 222 (1991) p. 617-646.
- Soldini, L., Piattella, A., Brocchini, M., Mancinelli, A. e Bernetti, R. Macrovortices-induced horizontal mixing in compound channels, *Ocean Dynamics*, 54, 333 – 339, 2004.
- Townsend, A. A., *The structure of turbulent shear flow*. Cambridge University Press, Cambridge, England, 1976, pp. 188-230.
- Wu, X. and Trupp, A. C., Spectral measurements and mixing correlations in a simulated rod bundle subchannels, *Int. J. Heat Transfer*, 37, 1277-1281, 1994.
- Yang, W. B., Zhang, H. Q., Chan, C. K., Lau, K. S., Lin, W. Y., Investigation of plane mixing layer using large eddy, *Computational Mechanics*, 34, 423 – 429, 2004.